Quantum Electronics **48** (12) 1113–1117 (2018)

https://doi.org/10.1070/QEL16842

Comparison of mode-locking regimes in a holmium fibre laser

S.A. Filatova, V.A. Kamynin, N.R. Arutyunyan, A.S. Pozharov, E.D. Obraztsova, P.A. Itrin, V.B. Tsvetkov

Abstract. **A comparison has been performed for two mode-locking regimes in an all-fibre holmium laser: locking due to nonlinear polarisation rotation (NPR) and hybrid mode-locking (NPR with application of single-walled carbon nanotubes). The characteristics of pulsed lasing in both regimes are investigated. Pulsed lasing is obtained at wavelengths of 2072 and 2082 nm, with FWHM values of 3.7 and 3.3 nm, respectively. The pulse width in both cases does not exceed 1.5 ps. The pulse energies in the NPR mode-locking and hybrid mode-locking regimes are 0.4 and 0.3 nJ, respectively. It is shown that the signal-to-noise ratio in the case of hybrid mode-locking is 3 dB better than that implemented under conditions of NPR mode-locking. A possibility of self-starting a laser system by applying hybrid mode-locking is indicated.**

Keywords: *holmium fibre laser, mode-locking, nonlinear polarisation rotation, hybrid mode-locking, single-walled carbon nanotubes.*

1. Introduction

Compact laser sources of ultrashort pulses (USPs), emitting in the spectral range of 2–3 μm, are of interest for solving both scientific and applied problems. These sources can be used as master oscillators (MOs) for nonlinear frequency conversion into the mid-IR and THz ranges [1, 2] and as MOs for bulk amplifiers [3]. The presence of water absorption peaks in the range of 2 μm makes these sources applicable for medical applications, for example, in dermatology and surgery [4]. They can also be used in materials processing [5], laser location [6], gas scanning [7] and atmospheric communication [8]. Among silica-based optical fibres, the largest lasing wavelengths are provided by optical fibres doped with holmium ions (Ho^{3+}), which have a wide gain band: 2000–2200 nm [9]. Thus, the development and implementation of compact holmium fibre lasers generating ultrashort pulses is an urgent problem.

Pulses shorter than 100 ps can be generated in the mode-locking regime. To date, in most of publications devoted to pulsed holmium fibre lasers, the mode-locking regime was implemented using saturable absorbers, such as carbon nanotubes [10], graphene [11, 12], black phosphorus [13], and semiconductor saturable absorber mirrors (SESAMs) [14, 15]. The mode-locking regime was also implemented using nonlinear polarisation rotation (NPR), which is due to the nonlinear Kerr effect in optical fibres [16, 17]. It should be noted that, when working with NPR-based pulsed lasers, there are difficulties related to self-starting of the laser system. To solve this problem, two saturable absorbers (fast and slow) are combined in the laser cavity [18] to implement hybrid mode-locking. The slow saturable absorber (with a response time of 300–700 fs), having a low saturation threshold, initiates mode-locking. The fast absorber based on the Kerr effect or NPR (the so-called artificial saturable absorber), which has a short response time (about 10 fs), efficiently forms pulses. The hybrid mode-locking is actively used in erbium [19, 20] and thulium [21, 22] fibre lasers. An NPR-based scheme of holmium fibre laser was supplemented with a saturable absorber mirror in [16]. Thus, hybrid mode-locking was obtained, and a possibility of self-starting was implemented for the system. However, this scheme contained bulk elements and could not be considered as an all-fibre one.

Thus, it is of interest to compare (under identical conditions) different mode-locking regimes (NPR and hybrid mode-locking) in an all-fibre holmium laser and analyse the parameters of the pulsed radiation obtained.

2. Experimental setup

Figure 1 shows a schematic of the experimental setup based on a hybrid mode-locked all-fibre holmium laser. The pump radiation source was a cw fibre laser based on ytterbium (Yb) GTWave fibre, operating at a wavelength of 1125 nm. The choice of this pump wavelength was determined by the occurrence of the $^5I_8 \rightarrow {}^5I_6$ transition in holmium ions and the spectral dependence of the Yb laser efficiency. The ytterbium lasers based on GTWave fibre exhibit a sharp drop of the lasing efficiency at wavelengths longer than 1120 nm [23]. Therefore, we used a wavelength of 1125 rather than 1150 nm in most experiments with holmium fibre lasers in order to obtain a sufficiently high lasing efficiency. The cw Yb fibre laser had a power of 8 W; however, the power used to pump the holmium fibre laser did not exceed 3.3 W. The pump radi-

S.A. Filatova, V.A. Kamynin, A.S. Pozharov Prokhorov General Physics Institute, Russian Academy of Sciences, ul. Vavilova 38, 119991 Moscow, Russia; e-mail: filsim2910@gmail.com;
N.R. Arutyunyan, V.B. Tsvetkov Prokhorov General Physics Institute, Russian Academy of Sciences, ul. Vavilova 38, 119991 Moscow, Russia; National Research Nuclear University 'MEPhI' (Moscow Engineering Physics Institute), Kashirskoe sh. 31, 115409 Moscow, Russia;
E.D. Obraztsova Prokhorov General Physics Institute, Russian Academy of Sciences, ul. Vavilova 38, 119991 Moscow, Russia; Moscow Institute of Physics and Technology, Institutskii per. 9, Dolgoprudnyi, 141701 Moscow region, Russia;
P.A. Itrin Ulyanovsk State University, ul L. Tolstogo 42, 432017 Ulyanovsk, Russia

Received 9 October 2018; revision received 17 October 2018
Kvantovaya Elektronika **48** (12) 1113–1117 (2018)
Translated by Yu.P. Sin'kov

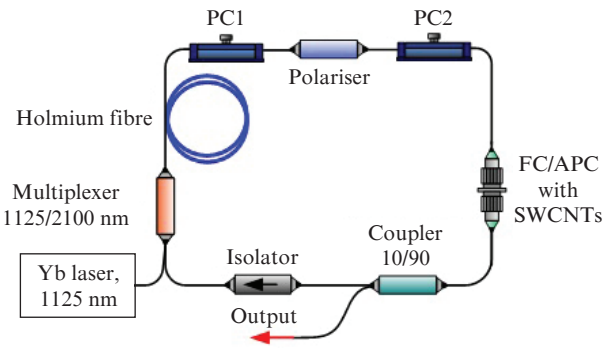

Figure 1. Schematic of a hybrid mode-locked holmium fibre laser (PC1 and PC2 are polarisation controllers; SWCNTs are single-walled carbon nanotubes).

ation arrived at the ring cavity of the holmium laser (about 14 m long) through a fibre multiplexer, operating in the range of 1125/2100 nm.

The laser ring cavity consisted of a holmium fibre ~6 m long and a single-mode SMF-28e fibre about 8 m long. The active fibre was prepared by the MCVD technology; its parameters were as follows: the difference between the core and cladding refractive indices was 0.007, the core diameter was 16 μm, and the cutoff wavelength was about 2 μm. The concentration of holmium ions in the fibre was 5×10^{19} cm^{-3}, and the fibre absorption at the pump wavelength (1125 nm), measured by the break method, was 5 dB m^{-1}. The active 6-m-long fibre was applied to obtain as large wavelength as possible. Experiments were performed in [24], where the radiation wavelength was changed as a function of the active-fibre length in the cavity. The total intracavity dispersion of the laser, calculated from the formula reported in [17, 25], turned out to be about −1.5 ps^2. The group-velocity dispersion (β_2) at a wavelength of 2080 nm for the single-mode SMF-28e fibre was −0.102 ps^2 m^{-1} [26]. Having known the group-velocity dispersion of the cavity and single-mode fibre, as well as the length of the fibre in use, one can calculate the dispersion β_2 for the holmium fibre; it was found to be −0.112 ps^2 m^{-1}.

A fibre isolator operating in the vicinity of 2 μm was used to select one propagation direction for generated radiation. The radiation loss in the forward and backward directions were, respectively, 0.6 and more than 30 dB. The NPR mode-locking regime was implemented with the aid of a fibre polariser and two polarisation controllers. To implement hybrid mode-locking in the scheme of an NPR-based laser, a transparent carboxymethylcellulose (CMC) film with homogeneously dispersed single-walled carbon nanotubes (SWCNTs), which played the role of a slow saturable absorber, was inserted between FC/APC optical connectors.

The fabrication technology and characteristics of SWCNT suspensions in 1% aqueous CMC solution were described in detail in [27, 28]. Cellulose was chosen to be the key element because it is simultaneously an effective surfactant and a matrix material. In this context, one needs only two elements (CMC and SWCNTs) to prepare a suspension for fabricating high optical quality films. Since cellulose is a highly flexible polymer, one can form thin (4–6 μm) films from it after drying the suspension. Such films have already been used in erbium- and thulium-doped fibre lasers [29, 30]. The largest lasing wavelength achieved in [30] was 1.9 μm. The centre wavelength of holmium fibre laser used in this study was red-shifted (to 2080 nm); therefore, we applied commercial TuBall nanotubes with a large diameter (more than 2 nm). Figure 2 shows the transmission spectrum of an SWCNT-containing film used in our experiments. The absorption near ~2600 nm is related to the E_{11} transition in the SWCNT density of states. The width of this transition is sufficient to implement mode-locking at a wavelength of 2082 nm. The absorption bandwidth is determined by the distribution of nanotube diameters.

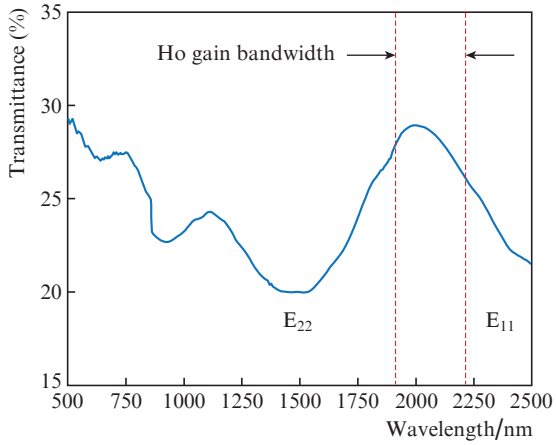

Figure 2. Transmission spectrum of a carboxymethylcellulose film with homogeneously dispersed SWCNTs.

A fibre coupler with a coupling ratio of 9/1 was used as an output of radiation from the laser cavity and provided 90% output of laser power. The scheme of an NPR mode-locked holmium fibre laser differed only by the absence of an SWCNT-containing film between the optical connectors.

The laser characteristics were analysed using the following equipment: optical spectrum analyser (Avesta ASP-IR-2.6), digital spectrum analyser with a bandwidth of 3 GHz (Gwinstek GSP-7830), 60-MHz photodiode, oscilloscope [Tektronix TDS 2022C (200 MHz)], and scanning autocorrelator (Avesta AA-20DD).

3. Experimental results

To compare the lasing characteristics in different mode-locking regimes, we first analysed the characteristics for an NPR mode-locked holmium laser. Then an SWCNT-containing film was inserted between optical connectors, and the corresponding characteristics were investigated for the holmium laser operating in the hybrid mode-locking regime. Then the lasing characteristics obtained in different mode-locking regimes were compared.

Stable pulsed lasing due to NPR was implemented at a pump power of 3 W, whereas for the hybrid mode-locking regime the lasing threshold increased, and the pump power necessary for pulsed lasing turned out to be 3.3 W. The average lasing power in the NPR and hybrid mode-locking regimes was 6.4 and 4.7 mW, respectively. Figure 3 shows the emission spectra of a pulsed holmium fibre laser operating in different regimes. Both spectra have a typical shape with Kelley peaks, which are characteristic of soliton lasing and are formed due to the spectral interference between the soliton

and dispersive waves [31]. It can be seen in Fig. 3 that different regimes are characterised by different values of the central lasing wavelength and full width at half maximum (FWHM): they are, respectively, 2072 and 3.7 nm in the case of NPR mode-locking and 2082 and 3.3 nm for hybrid mode-locking.

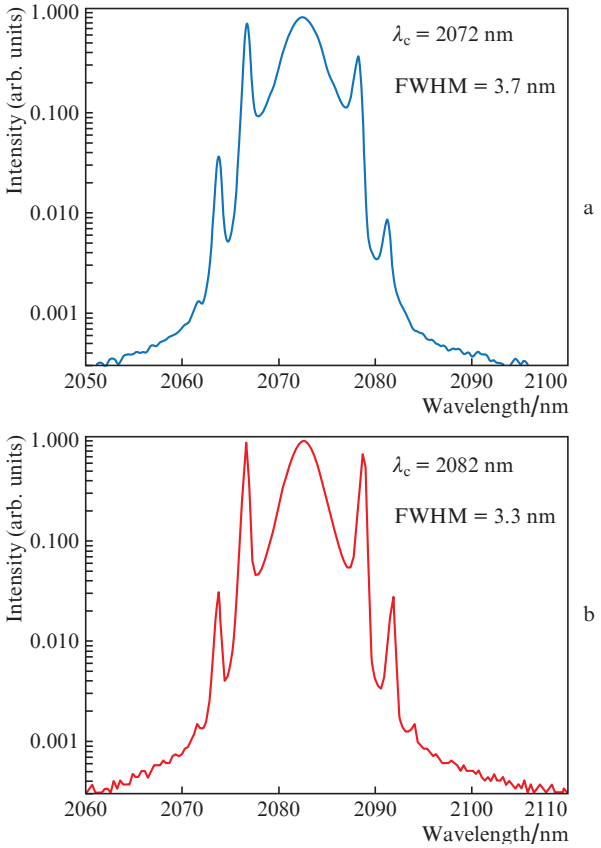

Figure 3. Lasing spectra of a holmium fibre laser operating in the (a) NPR and (b) hybrid mode-locking regimes.

The pulse width was measured with a scanning autocorrelator according to the scheme presented in Fig. 4. A polarisation controller was used to control the lasing polarisation, because the autocorrelator sensitivity depends on this parameter. Since the autocorrelator has a fibre input, radiation was introduced into the scheme via an FC/PC optical connector. To prevent the reflected radiation from entering the laser ring cavity, the scheme was supplemented with a fibre isolator, identical to that placed in the cavity. The single-mode fibre used in this scheme was 0.7 m long.

The measured autocorrelation functions (ACFs) are shown in Fig. 5. For the NPR mode-locked laser, the pulse width was found to be 1.2 ps. In the case of hybrid mode-locking

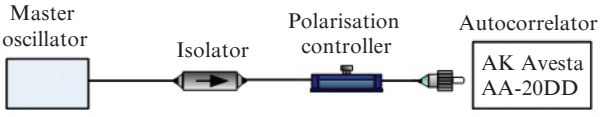

Figure 4. Schematic for measuring the laser pulse width.

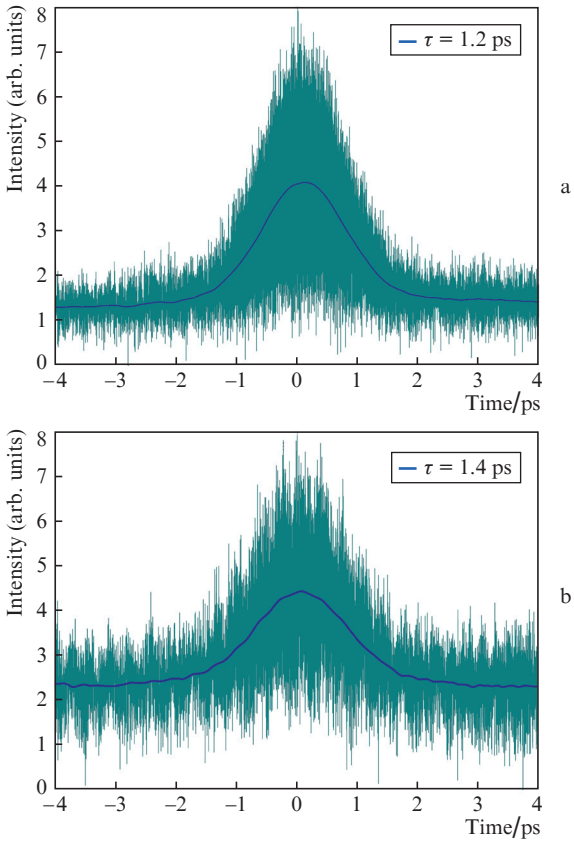

Figure 5. Autocorrelation functions for the pulses generated by a holmium fibre laser operating in the (a) NPR and (b) hybrid mode-locking regimes.

(Fig. 5b), the ACF is fairly noisy; this fact indicates that measurements were performed at the autocorrelator sensitivity threshold. The pulse width was 1.4 ps in this case. In both regimes, the pulse width corresponds to the FWHM value.

The pulse repetition frequency was 14.9 MHz, a value corresponding to the cavity length ($\sim$ 14 m). The pulse sequences for the mode-locking regimes under consideration are shown in Fig. 6. The difference in these oscillograms is that the fluctuations of pulse amplitudes in the case of NPR mode-locking (Fig. 6a) are much larger than for hybrid mode-locking (Fig. 6b).

Figure 7 shows the RF spectra at the laser fundamental frequency. It can be seen that the signal-to-noise ratio for the hybrid mode-locked laser is 3 dB better than that for the NPR mode-locked laser.

The lasing characteristics of a holmium fibre laser operating in different mode-locking regimes are compared in Table 1.

Note that the start of a laser operating in the hybrid mode-locking regime differs from that for an NPR mode-locked laser. To obtain pulsed lasing in the case of NPR mode-locking, the pump power should be first increased above the operating value and then (after the pulsed lasing occurrence) reduced (in order to exclude related continuous wave lasing). In turn, the first start of a hybrid mode-locked laser implies polarisation controller adjustment; however, during further switching on, the laser starts operating without any adjustment of the polarisation controller or pump power. We believe this can be considered as a self-starting system.

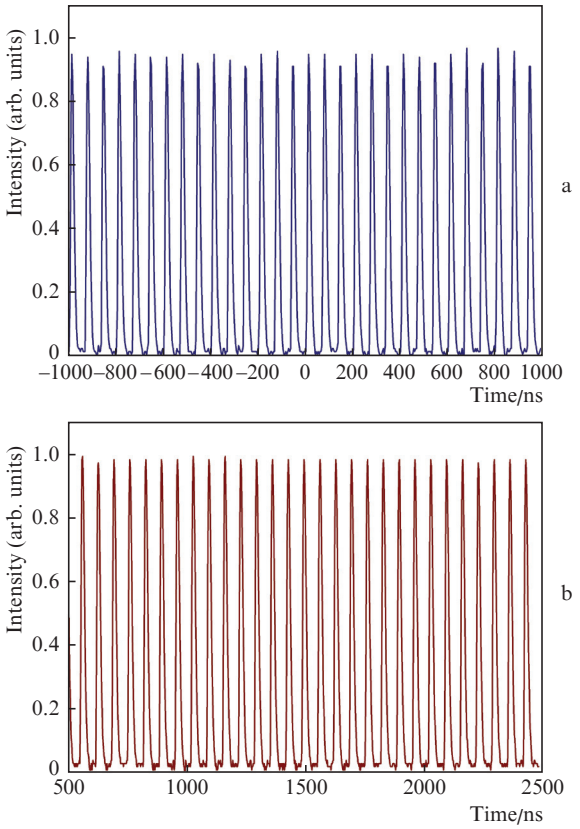

Figure 6. Pulse sequences generated by a holmium fibre laser operating in the (a) NPR and (b) hybrid mode-locking regimes.

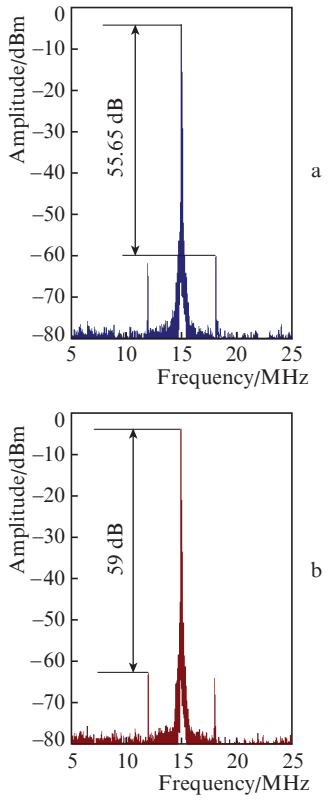

Figure 7. RF emission spectra of a holmium fibre laser operating in the (a) NPR and (b) hybrid mode-locking regimes.

Table 1.

Lasing characteristics	NPR mode-locking	Hybrid mode-locking
λ/nm	2072	2082
Spectrum FWHM/nm	3.7	3.3
Pulse repetition frequency/MHz	14.9	14.9
Pulse width/ps	1.2	1.4
$\langle P \rangle$/mW	6.4	4.7
P_{peak}/W	358	220
Energy/nJ	0.4	0.3

4. Conclusions

Different mode-locking regimes (NPR and hybrid-mode-locking), implemented in an all-fibre holmium laser, were compared under identical conditions. The pulsed lasing characteristics were analysed. Pulsed lasing at wavelengths of 2072 and 2082 nm with FWHM values of 3.7 and 3.3 nm, respectively, was demonstrated. The pulse widths for the NPR and hybrid mode-locking regimes were, respectively, 1.2 and 1.4 ps; the corresponding pulse energies were 0.3 and 0.4 nJ. Hybrid mode-locking is characterised by a better signal-to-noise ratio. A possibility of self-starting of a hybrid mode-locked laser system is indicated.

Acknowledgements. This work was supported by the Presidium of the Russian Academy of Sciences in terms of Basic Research Programme No. I.7 (Actual Problems of Photonics, Sensing of Inhomogeneous Media and Materials) and by the Russian Science Foundation (Project No. 14-22-00243).

References

1. Leindecker N., Marandi A., Byer R.L., Vodopyanov K.L., Jiang J., Hartl I., Fermann M., Schunemann P.G. *Opt. Express*, **20** (7), 7046 (2012).
2. Imeshev G., Fermann M.E., Vodopyanov K.L., Fejer M.M., Yu X., Harris J.S., Bliss D., Lynch C. *Opt. Express*, **14** (10), 4439 (2006).
3. Malevich P., Andriukaitis G., Flöry T., Verhoef A.J., Fernández A., Ališauskas S., Pugžlys A.,Baltuška A., Tan L.H., Chua C.F., Phua P.B. *Opt. Lett.*, **38** (15), 2746 (2013).
4. Serebryakov V.A., Boĭko É.V., Petrishchev N.N., Yan A.V. *J. Opt. Technol.*, **77** (1), 6 (2010).
5. Gattass R.R., Mazur E. *Nature Photon.*, **2** (4), 219 (2008).
6. Cariou J.P., Augere B., Valla M. *Comptes Rendus Phys.*, **7** (2), 213 (2006).
7. Walsh B.M. *Laser Phys.*, **19** (4), 855 (2009).
8. Li Z., Heidt A.M., Daniel J.M.O., Jung Y., Alam S.U., Richardson D.J. *Opt. Express*, **21** (8), 9289 (2013).
9. Hemming A., Simakov N., Haub J., Carter A. *Opt. Fiber Technol.*, **20** (6), 621 (2014).
10. Chamorovskiy A.Y., Marakulin A.V., Kurkov A.S., Okhotnikov O.G. *Laser Phys. Lett.*, **9** (8), 602 (2012).
11. Sotor J., Pawliszewska M., Sobon G., Kaczmarek P., Przewolka A., Pasternak I., Cajzl J., Peterka P., Honzátko P., Kašík I., Strupinski W., Abramski K. *Opt. Lett.*, **41** (11), 2592 (2016).
12. Dvoyrin V., Tolstik N., Sorokin E., Sorokina I., Kurkov A. *Proc. CLEO: 2015* (Munich, OSA, 2015) paper CJ_7_4.
13. Pawliszewska M., Ge Y., Li Z., Zhang H., Sotor J. *Opt. Express*, **25** (15), 16916 (2017).
14. Tolstik N., Sorokin E., Bugar I., Sorokina I.T. *Proc. Conf. "High-Brightness Sources and Light-Driven Interaction"* (Long Beach, US, OSA, 2016) paper MM6C-4.
15. Chamorovskiy A., Marakulin A.V., Ranta S., Tavast M., Rautiainen J., Leinonen T., Kurkov A.S., Okhotnikov O.G. *Opt. Lett.*, **37** (9), 1448 (2012).

16. Li P., Ruehl A., Bransley C., Hartl I. *Laser Phys. Lett.*, **13** (6), 065104 (2016).
17. Filatova S.A., Kamynin V.A., Zhluktova I.V., Trikshev A.I., Tsvetkov V.B. *Laser Phys. Lett.*, **13** (11), 115103 (2016).
18. Kurtner F.X., Der Au J.A., Keller U. *IEEE J. Sel. Top. Quantum Electron.*, **4** (2), 159 (1998).
19. Dvoretskiy D.A., Sazonkin S.G., Orekhov I.O., Kudelin I.S., Pnev A.B., Karasik V.E., Denisov L.K., Lyapin S.G., Davydov V.A. *Proc. Conf. "Progress In Electromagnetics Research Symposium-Spring" (PIERS)* (St. Petersburg, Russia, IEEE, 2017) pp 1598–1600.
20. Chernysheva M., Al Araimi M., Kbashi H., Arif R., Sergeyev S.V., Rozhin A. *Opt. Express*, **24** (14), 15721 (2016).
21. Chernysheva M.A., Krylov A.A., Mou C., Arif R.N., Rozhin A.G., Rümmelli M.H., Turitsyn S.K., Dianov E.M. *IEEE J. Sel. Top. Quantum Electron.*, **20** (5), 425 (2014).
22. Chernysheva M., Bednyakova A., Al Araimi M., Howe R.C., Hu G., Hasan T., Gambetta A., Galzerano G., Rümmelli M., Rozhin A. *Sci. Rep.*, **7**, 44314 (2017).
23. Kurkov A.S. *Laser Phys. Lett.*, **4** (2), 93 (2006).
24. Kamynin V.A., Filatova S.A., Zhluktova I.V., Tsvetkov V.B. *Quantum Electron.*, **46** (12), 1082 (2016) [*Kvantovaya Elektron.*, **46** (12), 1082 (2016)].
25. Kadel R., Washburn B.R. *Appl. Opt.*, **51** (27), 6465 (2012).
26. Pawliszewska M., Martynkien T., Przewłoka A., Sotor J. *Opt. Lett.*, **43** (1), 38 (2018).
27. Krylov A.A., Sazonkin S.G., Arutyunyan N.R., Grebenyukov V.V., Pozharov A.S., Dvoretskiy D.A., Obraztsova E.D., Dianov E.M. *JOSA B*, **33** (2), 134 (2016).
28. Chernysheva M.A., Krylov A.A., Arutyunyan N.R., Pozharov A.S., Obraztsova E.D., Dianov E.M. *IEEE J. Sel. Top. Quantum Electron.*, **20** (5), 448 (2014).
29. Tausenev A.V., Obraztsova E.D., Lobach A.S., Chernov A.I., Konov V.I., Kryukov P.G., Konyashchenko A.V., Dianov E.M. *Appl. Phys. Lett.*, **92** (17), 171113 (2008).
30. Solodyankin M.A., Obraztsova E.D., Lobach A.S., Chernov A.I., Tausenev A.V., Konov V.I., Dianov E.M. *Opt. Lett.*, **33** (12), 1336 (2008).
31. Kelly S.M. *Electron. Lett.*, **28** (8), 806 (1992).